

# Universal statistics of epithelial tissue topology

Abdulaziz Abdullah,<sup>1</sup> Demetris Avraam,<sup>1</sup> Oleksandr Chepizhko,<sup>2</sup> Thomas Vaccari,<sup>3</sup> Stefano Zapperi,<sup>4,5,6,7</sup> Caterina A. M. La Porta,<sup>8</sup> and Bakhtier Vasiev<sup>1,\*</sup>

<sup>1</sup>*Department of Mathematical Sciences, University of Liverpool, Liverpool, UK*

<sup>2</sup>*Institut für Theoretische Physik, Leopold-Franzens-Universität Innsbruck, Technikerstrae 21a, A-6020 Innsbruck, Austria*

<sup>3</sup>*Department of Biosciences, University of Milan, via Celoria 26, 20133 Milano, Italy*

<sup>4</sup>*Center for Complexity and Biosystems, Department of Physics, University of Milan, Via Celoria 16, 20133 Milano, Italy*

<sup>5</sup>*CNR - Consiglio Nazionale delle Ricerche, Istituto di Chimica della Materia Condensata e di Tecnologie per l'Energia, Via R. Cozzi 53, 20125 Milano, Italy*

<sup>6</sup>*ISI Foundation, Via Chisola 5, Torino, Italy*

<sup>7</sup>*Department of Applied Physics, Aalto University, P.O. Box 11100, FIN-00076, Aalto, Finland*

<sup>8</sup>*Center for Complexity and Biosystems, Department of Environmental Science and Policy, University of Milan, via Celoria 26, 20133 Milano, Italy*

Cells forming various epithelial tissues have a strikingly universal distribution for the number of their edges. It is generally assumed that this topological feature is predefined by the statistics of individual cell divisions in growing tissue but existing theoretical models are unable to predict the observed distribution. Here we show experimentally, as well as in simulations, that the probability of cellular division increases exponentially with the number of edges of the dividing cell and show analytically that this is responsible for the observed shape of cell-edge distribution.

Epithelial tissues are commonly represented by unicellular layers and have quite distinctive topological features [1, 2]. Cells, as seen from the tissue surface, represented by polygons (Figure 1a) whose number of edges (or the number of neighboring cells) usually varies between 4 and 9 (Figure 1b). Triangular cells or cells with ten or more edges are rarely met. Histograms displaying the fraction of cells with a given number of edges, cell-edges distribution histograms (CEDH), are commonly used to describe the topology of epithelial tissue [3, 4] and display a remarkable degree of universality across experiments and species [5]. CEDH indicates that the majority of the cells in an epithelial tissue have hexagonal topology ( $\sim 45\%$ ), pentagonal and heptagonal cells are observed less frequently ( $\sim 25\%$  and  $\sim 20\%$  respectively) while 4-, 8- and 9-sided cells are rarely observed with a frequency of less than 10% in total (Figure 1c).

A few mathematical models have been developed to explain the universal shape of the observed CEDHs. The model introduced by Gibson et al. [1] (thereafter referred to as the GPNP model), considers cellular proliferation as the sole process responsible for tissue topology. Hence, the number of cell edges is defined when the cell is born, does not change during its growth, but can be affected by the division of neighboring cells. According to the GPNP model, cells are polygons with four or more edges and are divided synchronously in discrete generations, ignoring any spatial correlation between the number of edges of the neighboring cells. The GPNP model reproduces fairly well the observed CEDHs with the only exception that 4-sided cells do completely disappear. Sandersius et al. [5] attempted to revisit the GPNP model to overcome the shortcoming with the 4-sided cells. They have developed four modifications of the GPNP model but none of

them was successful: it turned out that all considered modifications of the GPNP destroy the shape of CEDH and it becomes not comparable with the CEDHs from experiments. The authors concluded that their models fail because they do not take into account spatial correlations between sidedness of neighbouring cells (so called Aboav's law [6]) which should play a significant role on the development of a proliferating tissue. They confirmed this conclusion by showing a good agreement between experimental observations and simulations of a computational subcellular element model [7] although the analytical confirmation was omitted.

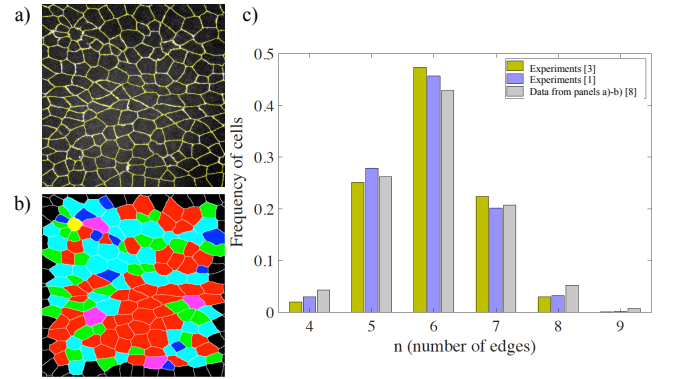


FIG. 1: a) A segmented image of the tissue formed by a *drosophila* pupa [8]. b) The same image as in a) is colored according to the number of edges in each cell (blue:4, green:5, red:6, cyan:7, yellow:8). c) The corresponding histogram averaged over three different experiments and different time steps. The histograms are compared with earlier results reported in the literature [1, 3]

In this letter, we propose mathematical models based

on master equations that describe the evolution of the CEDH due to cellular proliferation and changes in cell shapes. We use these models to identify key features of tissue dynamics responsible for the experimentally observed CEDH. We show that in order to be successful, a model of growing tissue should account for the fact that cells with more edges divide more frequently. This fact is fully justified: cells mature before dividing and matured cells have usually more edges. Using experiments on *drosophila* and numerical simulations on a dynamic vertex model, we find that the frequency of cellular division increases exponentially with the number of cell edges. Furthermore, we model the effect of cellular shape changes (due to T1-transitions as illustrated in Figure 2b) and show that this also allows to reproduce the universal cell-edge distribution.

For experimental comparison, we consider time lapse images obtained during the development of *drosophila* pupae (see Ref. [8] for experimental details). The determination of the number of edges is done by a custom Matlab code. Initial image segmentation is performed by a watershed algorithm with some preliminary adjustments of the image brightness. Then image segmentation is improved manually (see Figure 1a). We identify the region corresponding to each cell and count its neighbors (see Figure 1a). Cells touching the boundary of the image are excluded from the analysis. In this way, we are able to obtain the CEDH (see Figure 1c) which is in agreement with earlier observations [1, 5].

In our first model we consider a growing tissue where the CEDH is only affected by cellular proliferation while growing cells do not change their shapes as in Ref. [1]. To write the master equation, we denote by  $N(t)$  the total number of cells at time  $t$ ;  $N_i(t)$  the number of  $i$ -sided cells, and  $p_i(t) = N_i(t)/N(t)$  the fraction of  $i$ -sided cells in the population. We also assume that the number of edges cells can have varies from 4 to 9. The rate of change in the fraction of  $i$ -sided cells is given by

$$\frac{d}{dt} \left( \frac{N_i}{N} \right) = \frac{dN_i N - N_i dN}{N^2 dt} = \frac{dN}{N dt} \left( \frac{dN_i}{dN} - \frac{N_i}{N} \right),$$

which can be written as

$$\dot{p}_i = \alpha (M_i + K_i - p_i), \quad (1)$$

where  $\alpha = \frac{dN}{N dt}$  is the cells proliferation rate and the expression in brackets defines the probability for  $i$ -sided cell to appear/disappear in a single proliferation event.  $\frac{dN_i}{dN} = M_i + K_i$  is split into two terms, where  $K_i$  determines the changes due to removal of  $i$ -sided mother cells and addition of  $i$ -sided daughter cells while  $M_i$  accounts for the changes in the number of edges of neighboring cells after each division. The term  $K_i$  is easy to estimate assuming that the fraction of  $i$ -sided cells in the neighborhood of any dividing cell is equal to their total fraction (i.e. there is no spatial correlation). Then:

$$K_i = -2p_i + 2p_{i-1}, \quad (2)$$

where the first term defines the decrease in the fraction of  $i$ -sided cells if either or both affected neighbours were  $i$ -sided before the division and become  $i + 1$ -sided after the division, and the second term counts the cells that were  $i - 1$ -sided before the division and become  $i$ -sided. If we allow for the number of edges to vary from four to nine, then Eq. (2) holds for  $5 < i < 8$ , while for the boundary cases we have  $K_4 = -2p_4$  and  $K_9 = 2p_8$ .

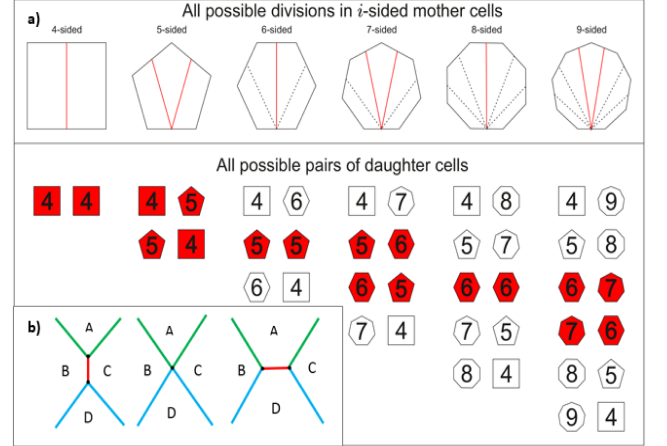


FIG. 2: a) All possible divisions in  $i$ -sided mother cells and the corresponding combinations of daughter cells. The red lines in the upper panel and the red colored pairs of daughter cells at the lower panel denote the division patterns and the possible pairs of daughter cells under the ‘equal split division’ scenario [9]. b) Three consecutive images illustrating a T1-transition in dynamic tissue: the edge AD disappears, while the new BC edge forms.

The term  $M_i$  in Eq. (2) describes changes associated with the replacement of a mother cell by two daughter cells during cell division. In the following, we only consider division events (as listed in [9]) where the mother cell is split into two approximately equal daughter cells. Hence, we assume that a mother cell with an even number of edges divides into two daughter cells with equal number of edges, while a mother cell with an odd number of edges splits into cells that differ by one in their number of edges. Allowed divisions are illustrated in red in the upper panel of Figure 2a and possible pairs of daughter cells - in red in the lower panel of Figure 2a. It is easy to see that  $i$ -sided daughter cells can only appear after the division of  $(2i - 3)$ ,  $(2i - 4)$  or  $(2i - 5)$ -sided cells. Then, the term  $M_i$  can be represented as:

$$M_i = \begin{cases} 2p_{2i-4}^* + p_{2i-3}^* - p_i^* & \text{if } i = 4 \\ p_{2i-5}^* + 2p_{2i-4}^* + p_{2i-3}^* - p_i^* & \text{if } 4 < i < 7 \\ p_{2i-5}^* - p_i^* & \text{if } i = 7 \\ -p_i^* & \text{if } i > 7 \end{cases} \quad (3)$$

where  $p_i^*$  is the probability that a mother cell, in a randomly chosen division, is  $i$ -sided. If, following [1], we

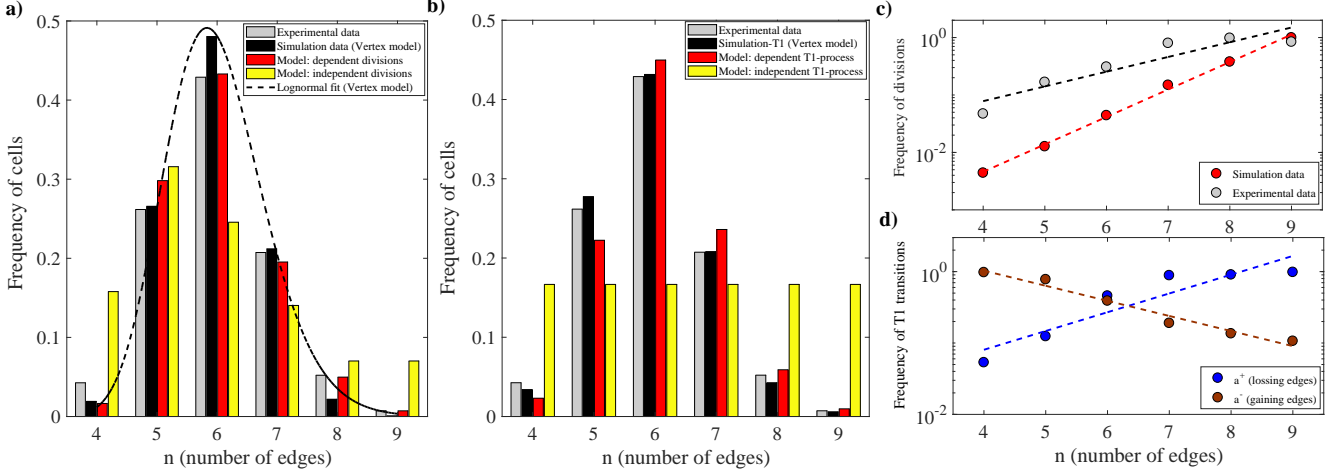


FIG. 3: a) CEDHs from simulations and analytical models (neglecting/considering dependence of the probability of cellular division on the number of edges) of growing tissue (compared with experimental CEDH). b) CEDHs from simulations and analytical models (neglecting/considering dependence of the probability of T1-transition on the number of edges) of dynamic tissue (compared with experimental CEDH). c) Fractions,  $\sigma_n$ , of dividing  $n$ -sided cells as estimated from the experimental images (data from [8] analyzed here) and from numerical simulations using the vertex model. In both cases, the probability of division grows exponentially with the number of cell edges. d) Fractions of  $n$ -sided cells gaining ( $a_n^+$ ) and loosing ( $a_n^-$ ) an edge in course of T1-transitions as obtained from numerical simulations using the vertex model.

assume that all cells divide with equal probability, i.e.  $p_i^* = p_i$ , then Eqs. (1-3), form a system of linear equations satisfying the condition  $\sum_{i=4}^9 p_i = 0$  and describing the evolution of CEDH. One can show that this system has one zero eigenvalue while all its other eigenvalues are negative so that its solution converges to the eigenvector corresponding to the zero-eigenvalue. This solution does not, however, reproduce the topology of growing tissue obtained experimentally (see Figure 3a).

The assumption of a cell division probability that is independent on the number of edges is not supported by experiments [2]. We show in Figure 3c that the division probability is increasing exponentially with the number of edges of the dividing cell. This result is expected considering that cells have to mature before they divide and the number of edges of long-living cell tends to increase due to the division of neighboring cells. We thus modify our model assuming that in Eq. (3) the probability that a dividing cell is  $i$ -sided is proportional to  $\sigma_i p_i$  where  $\sigma_i$  is estimated from experiments (Figure 3c), yielding

$$p_i^* = \frac{\sigma_i p_i}{\sum_i \sigma_i p_i}, \quad (4)$$

which makes our model nonlinear. Solutions of this model yield steady-state results for the distribution of cell edges that are now in excellent agreement with experimental observations as shown in Figure 3a.

As a further confirmation of the theoretical results, we perform numerical simulations using a dynamical vertex model [10] which is commonly used in modelling epithelial tissues [11, 12]. In this model, each cell is represented

by a polygon whose shape can change due to the forces acting on its vertices. Simulations of the vertex model are implemented through the open software Chaste [13], considering the formation of a tissue from a single cell in the course of successive divisions (see Supplementary Movie 1). The number of edges of each single cell (and the number of edges of its neighbors) can be explicitly specified and the process of division can be fully determined. We find that the CEDHs for simulated growing tissues converge and (when the number of cells exceeds 1000) acquire the shape shown by the black histogram in Figure 3a. Simulations also show that the probability of cellular division is exponentially increasing with the number of its edges (see Figure 3c). Both results are in excellent agreement with the experimental data.

In the model we have considered so far, we have assumed that the CEDH is affected only by cellular proliferation while the number of edges in growing daughter cells does not change, unless affected by dividing neighboring cells. Epithelial cells can, however, show dynamical changes in their shapes, manifested by the so-called T1-transitions [14] when one edge disappears (bringing together two distant cells) while another appears (separating two neighbouring cells) (see Figure 2b). We study the effect of T1-transitions on CEDH in simulations using a modified version of the dynamic vertex model. Cells in the simulation are not allowed to proliferate but forced to dynamically change and undergo T1-transitions (see Supplementary Movie 2). We note that T1-transitions do not change neither the number of cells nor the total number of cell edges, so that the outcome of these sim-

ulations strongly depends on the initial state of modeled tissue. Here we consider a tissue composed of a considerable amount of cells with six edges per cell on average, corresponding to the experimental case [2]. These simulations show that if we start with a tissue containing more than 100 hexagonal cells the CEDH evolves towards a stationary shape matching the experimental results (see Figure 3b).

We can explain this result theoretically by considering the master equation describing the dynamics of CEDH in a tissue without cell division:

$$\dot{p}_i = \alpha F_i, \quad (5)$$

where (similarly to Eq.(1))  $\alpha$  defines the rate at which T1-transitions take place and  $F_i$  defines the probability of appearance/disappearance of a  $i$ -sided cell in a single T1-transition event. To find  $F_i$ , we note that in each T1-transition two cells loose an edge and two other cells gain an extra edge so that

$$F_i = \begin{cases} -2p_i^+ + 2p_{i+1}^- & \text{if } i = 4 \\ 2p_{i-1}^+ - 2p_i^- - 2p_i^+ + 2p_{i+1}^- & \text{if } i = 5, \dots, 8 \\ 2p_{i-1}^+ - 2p_i^- & \text{if } i = 9 \end{cases} \quad (6)$$

where  $p_i^-$  and  $p_i^+$  are probabilities for  $i$ -sided cell to loose or gain an edge in course of a random T1-transition event. If we assume that all cells have the same probability to undergo a T1-transition then  $p_i^- = p_i^+ = p_i$ . In this case, Eqs (5-6) define a linear system whose solution converges to the eigenvector corresponding to its zero-eigenvalue. It can be shown analytically as well as numerically (by solving the system (5-6)) that all components of this eigenvector are equal yielding a uniform CEDH (see Figure 3b). which obviously doesn't match experimental data. Another reasonable assumption is that any existing edge can undergo T1-transitions with the same probability, leading to the conclusion that cells with more edges should loose edges more frequently. We have found frequencies at which cells with different sidedness gain or loose edges in simulations using the vertex model (see Figure 3d). The simulations have shown that indeed the probability that the cell gains/looses an edge decreases/increases with the number of its edges. We take this data into account by reconstructing Eq. (6) with adjusted probabilities for  $i$ -sided cells to gain/loose an edge:

$$p_i^+ = \frac{a_i^+ p_i}{\sum a_i^+ p_i}, \quad p_i^- = \frac{a_i^- p_i}{\sum a_i^- p_i}, \quad (7)$$

where the values of  $a_i^+$  and  $a_i^-$  are taken from the plot in Figure 3d. The histogram representing the stationary solution of this model is now in a good agreement with experimental data (see Figure 3b).

In this study, we have addressed the universal topological features of epithelial tissues represented by the shape

of the CEDH. This shape (although only comprised by 5 bars) fits log-normal rather than normal distribution (see 3a) and this observation extends its universality to other objects, for example, to the distribution of sizes of crashed stones in iron/gold mines [15]. Another important observation is that according to this shape the epithelial cell has in average 6 edges [3]. This number also appears in models of growing tissues: each cell division leads to the formation of one extra cell and 6 extra edges, implying that 6 edges per cell should be present in large tissues. This coincidence points to the crucial role of cellular proliferation in CEDH as checked in GPNP model and its modifications [1, 5]. Our results suggest that the reason why these models do not completely succeed in reproducing the observed CEDHs is that they do not take into account correlations between the number of edges of a cell and its division probability. We find instead, experimentally as well as in simulations, that the probability of cell division (i.e. fraction of dividing  $i$ -sided cells) increases exponentially with the number of cell edges (Figure 3c). Finally, our numerical as well as analytical studies have shown that the T1-transitions taking place in dynamic tissue also support the formation of universal CEDH.

This work has been supported by the BBSRC grant BB/K002430/1 to BV.

---

\* Electronic address: B.Vasiev@liverpool.ac.uk

- [1] M. C. Gibson, A. B. Patel, R. Nagpal, and N. Perrimon, *Nature* **442**, 1038 (2006), 33748313224.
- [2] F. Lewis, *Anatomical Records* **38**, 341 (1928).
- [3] F. Lewis, *Anatomical Records* **33**, 331 (1926).
- [4] P. Sahlin and H. Jönsson, *PLoS ONE* **5** (2010).
- [5] S. A. Sandersius, M. Chuai, C. J. Weijer, and T. J. Newman, *PLoS ONE* **6** (2011).
- [6] S. N. Chiu, *Materials Characterization* **34**, 149 (1995).
- [7] S. A. Sandersius, C. J. Weijer, and T. J. Newman, *Physical Biology* **8**, 045007 (2011).
- [8] C. Besson, F. Bernard, F. Corson, H. Rouault, E. Reynaud, A. Keder, K. Mazouni, and F. Schweisguth, *Curr Biol* **25**, 1104 (2015).
- [9] A. B. Patel, W. T. Gibson, M. C. Gibson, and R. Nagpal, *PLoS Computational Biology* **5** (2009), 67650908906.
- [10] H. Honda and T. Nagai, *Journal of Biochemistry* **157**, 129 (2015).
- [11] R. Farhadifar, J. C. Röper, B. Aigouy, S. Eaton, and F. Jülicher, *Current Biology* **17**, 2095 (2007).
- [12] A. G. Fletcher, M. Osterfield, R. E. Baker, and S. Y. Shvartsman, *Biophysical Journal* **106**, 2291 (2014).
- [13] G. R. Mirams, C. J. Arthurs, M. O. Bernabeu, R. Bordas, J. Cooper, A. Corrias, Y. Davit, S.-J. Dunn, A. G. Fletcher, D. G. Harvey, et al., *PLoS Computational Biology* **9**, e1002970 (2013).
- [14] T. Nagai and H. Honda, *Philosophical Magazine Part B* **81**, 699 (2001).
- [15] A. N. Kolmogorov, *Dokl. Akad. Nauk SSSR* **31**, 99 (1941).